

Observations and Analysis of a Detached Eclipsing Binary, V385 Camelopardalis

Ronald G. Samec

Faculty Research Associate, Pisgah Astronomical Research Institute, 1 PARI Drive, Rosman, NC 28772; ronaldsamec@gmail.com

Daniel B. Caton

Dark Sky Observatory, Physics and Astronomy Department, Appalachian State University, 525 Rivers Street, Boone, NC 28608-2106; catondb@appstate.edu

Danny R. Faulkner

Johnson Observatory, 1414 Bur Oak Court, Hebron, KY 41048; dfaulkner@answersingenesis.org

Received July 16, 2019; revised September 4, 17, 2019; accepted September 17, 2019

Abstract V385 Cam is found to be a $G7 \pm 2$ type ($T \sim 5500$ K) pre-contact eclipsing binary. It was observed on December 15, 16, 17, and 18, 2017, at Dark Sky Observatory in North Carolina with the 0.81-m reflector of Appalachian State University. Three times of minimum light were determined from our present observations, which include two primary eclipses and one secondary eclipse. Twelve other minima were determined or found in the literature. This allowed an 18.5-year period study and a possible quadratic ephemeris was found. The resulting weak period decrease may indicate that the solar type binary is undergoing magnetic braking. A $BVR_c I_c$ simultaneous Wilson-Devinney Program (wd) solution gives a detached solution. This model has a primary component with a 96% fill-out and a secondary component with 91% fill-out. The solution has a mass ratio of 0.390 ± 0.001 , and a component temperature difference of ~ 1000 K. The large ΔT in the components verifies that the binary is not yet in contact. Two hot spots were used in the modeling, a polar spot and a smaller southern spot with a 120° colatitude. The binary star inclination is $\sim 84.1 \pm 0.2^\circ$, resulting in a total eclipse (secondary component) of 27.2 minutes in duration.

1. Introduction

In this paper, we continue our study of pre-contact W UMa binaries. Among those recently studied include AE Cas (Chamberlain *et al.* 2019), NSVS 103152 (Samec *et al.* 2018), TYC 1488-693-1 (Samec *et al.* 2018), NSVS 10083189 (Samec *et al.* 2017a), and GQ Cancri (Samec *et al.* 2017b), etc. We have designated these as pre-contact W UMa binaries since they are in detached or semidetached configurations and their orbital period studies have shown them to be systems that may be undergoing magnetic braking (angular momentum loss, AML). They could be evolving into contact and finally to binary coalescence and the formation of a fast rotating, earlier spectral type single star after a red novae event (Tylenda and Kamiński 2016). Streaming plasmas moving on stiff, rotating radial patterns away from the binary out to the Alfvén radius (~ 50 stellar radii) could cause this. Here we present the first precision photometry and light curve analysis of another such candidate, the pre-contact system V385 Cam. The first report of these observations was given as a poster paper at the American Astronomical Society Meeting #234 (Samec *et al.* 2019).

2. History

The variable was listed as a near contact binary by Shaw (1994) who gives the light curve (see Figure 1), magnitude ($V=13.78$), and ephemeris:

$$HJD = 2451396.798279 d + 0.61521068 \times E, \quad (1)$$

and position of the binary designated also as NSVS 00580289.

Khruslov (2006) included it in a list of New Short-Period Eclipsing Binaries in Camelopardalis (Figure 2). He gave the position, magnitude range ($V=13.65\text{--}14.20$), finding chart, light curve, the designation GSC 4515-00038, and the ephemeris:

$$HJD = 2451515.845 d + 0.61525 \times E. \quad (2)$$

The binary was listed in the “80th Name-List of Variable Stars, Part I” (Kazarovets *et al.* 2011).

This system was observed as a part of our student/professional collaborative studies of interacting binaries using data taken from Dark Sky Observatory (DSO) observations. The observations were taken by R. Samec, D. Caton, and D. Faulkner. Reduction and analyses were done by R. Samec. The GAIA DR2 determined distance is 854 ± 13 pc (Bailer-Jones 2015). The patrol light curve shown in Figure 3 is taken from the ASAS-SN, All-Sky Automated Survey for Supernovae Variable Stars Data Base (Shappee *et al.* 2014; Kochanek *et al.* 2017; <https://asas-sn.osu.edu>). In addition, V385 Cam has a $J-K=0.22$, an ephemeris:

$$JD_{\text{HelMIN}} I = 2457386.76033 + 0.6152709 \times E, \quad (3)$$

and catalog name: ASASSN-V J051947.00+773613.3.

3. $BVR_c I_c$ photometry

Our 2017 $BVR_c I_c$ light curves were taken by D. Caton on December 15, 16, 17, and 18, 2017, at Dark Sky Observatory

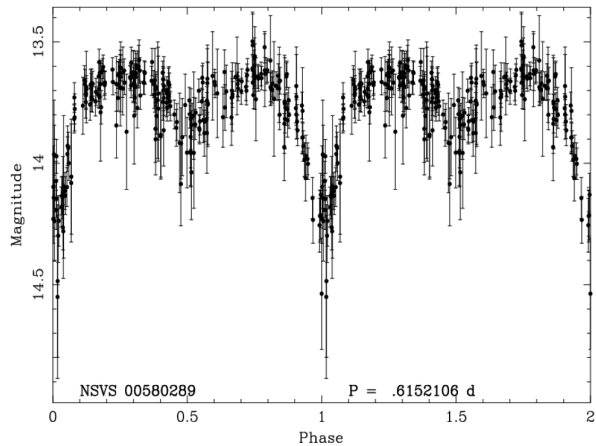


Figure 1. Light curves of V385 Cam (Shaw 1994; <http://www.physast.uga.edu/~jss/nch/>).

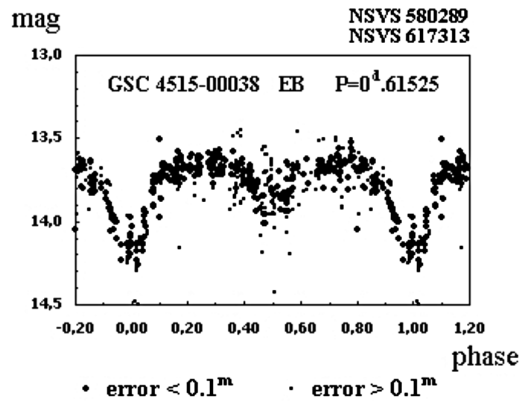


Figure 2. Light curve from Khruslov *et al.* (2006).

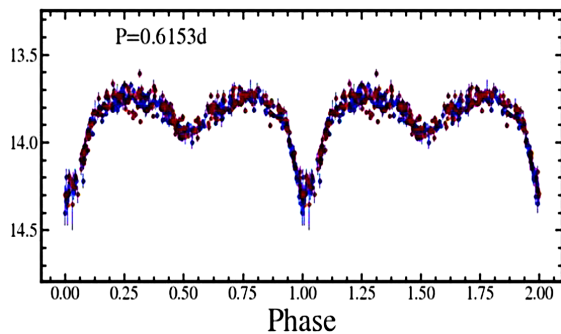


Figure 3. V light curves of V385 Cam (<https://asas-sn.osu.edu/>).

Table 1. Information on the stars used in this study.

Star	Name	R.A. (2000) h m s	Dec. (2000) ¹ ° ' "	V ²	J-K ³
Variable (V)	V385 Cam GSC 4515-00038 2MASS J05194709+7736136 ASASSN-V J051947.00+773613.3 Gaia DR2 552348118709696256	05 19 47.0833	+77 36 13.637	13.78	0.452 ± 0.046
Comparison (C)	GSC 4515 626 3UC 336-015704	05 19 49.3367	+77 33 38.989	13.334	0.34
Check (K)	GSC 4515 1148	05 19 13.0678	+77 36 18.970	11.97	0.593 ± 0.041

¹ UCAC3 (U.S. Naval Obs. 2012), ² APASS (Henden *et al.* 2015), ³ 2MASS (Cutri *et al.* 2003).

in North Carolina with the 0.81-m reflector of Appalachian State University at Philips Gap, North Carolina, with a thermoelectrically cooled (-40°C) 2KX2K Apogee Alta with standard BVR_cI_c filters.

Our observations included 347 images in the B filter, 369 images in the V filter, 319 images in the R_c filter, and 306 images in the I_c filter. The probable error of a single observation was 8 mmag in B, 7 mmag in V and I, and 6 mmag in R. Exposure times varied from 40 to 80s in B, 25–60s in V, and 15–40s in R_c and I_c , depending on the count needed to obtain 1% photometry. Photometric targets are given in Table 1.

The nightly C–K magnitudes stayed constant throughout the observing run with a precision of about 1% (see, for instance, Figure 4.). The observed curves from December 16, 2017, are shown in Figure 5.

The V–C differential color indices, $\Delta(\text{B} - \text{V})$ and $\Delta(\text{R}_c - \text{I}_c)$, are seen to be very close to zero. The finder chart is given as Figure 6 with the variable star (V), comparison star (C), and check star (K) shown. Our observations are listed in Table 2, with magnitude differences ΔB , ΔV , ΔR_c , and ΔI_c in the sense variable minus comparison star.

4. Orbital period study

Three times of minimum light were calculated, 2 primary and 1 secondary eclipses, from our present observations:

$$\begin{aligned} \text{HJD I} &= 2457372.62072 \pm 0.0003 \text{d}, \\ \text{HJD II} &= 2457372.92658 \pm 0.0011 \text{d}, \end{aligned}$$

A least squares minimization method (Mikulášek *et al.* 2014) was used to determine the minima for each curve, in $\text{B}, \text{V}, \text{R}_c$, and I_c . Eight times of low light were taken from a light curve phased from data (ASAS J051947,00+773613.3) from the All-Sky Automated Survey (ASAS; Pojmański 1997). This plot was used to get times of minima from parabola fits within ± 0.01 of phases 0.0 and 0.5 (https://asas-sn.osu.edu/database/light_curves/340255). The ASAS ephemeris provided another minimum. Another time of minimum light is given by Diethelm (2013). A linear ephemeris and quadratic ephemerides were determined from these data.

All of these times of minimum light are given in Table 3.

Both linear and quadratic ephemerides were determined from these data:

$$\text{JDHelMinI} = 2457372.61883 + 0.61527147 \times E \\ \pm 0.00057 \pm 0.00000014 \quad (4)$$

$$\text{JDHelMinI} = 2457372.61875 + 0.61527021 \times E - 0.00000000014 \times E^2 \\ \pm 0.00055 \pm 0.00000068 \pm 0.0000000007 \quad (5)$$

The residual plots for the linear and the quadratic ephemerides are shown in Figures 7a and 7b, respectively. The r.m.s. of the quadratic ephemeris is somewhat better. The higher quality points at the end of the plot cause one to admit of such a possibility. The period study covers a period of some 18.5 years and shows the possibility that the period may be decreasing (at about the ~ 1.5 sigma level, with the errors shown here are probable errors). This could be due to mass flow to the secondary component or magnetic braking from the solar components.

The quadratic ephemeris yields a $\dot{P} = -1.66 \times 10^{-7}$ d/yr, or a mass exchange rate of

$$\frac{dM}{dt} = \frac{\dot{P} M_1 M_2}{3P(M_1 - M_2)} = \frac{-5.28 \times 10^{-8} M_{\odot}}{d}. \quad (6)$$

in a conservative scenario. The possibility of a third component should be at least considered; the quadratic curve could be part of a sinusoid. In fact, a large number of short-period systems have third components (Tokovinin *et al.* 2006). Further eclipse timings are needed to confirm or disaffirm this whole scenario.

The O-C quadratic residual calculations are given in Table 3.

5. Light curves and light curve solution

The BVR_cI_c phased light curves calculated from Equation 3 are displayed in Figures 8a and 8b. The curves are of good precision, averaging somewhat better than 1% photometric precision. The amplitude of the light curve varies from 0.64 to 0.46 mag in B to I. The O'Connell effect, an indicator of spot activity, averages several times the noise level, 0.02–0.04 mag. The differences in minima are large, 0.22–0.45 mags, indicating noncontact light curves. The B–V color curves fall ever so very slightly at phase 0.0, however, the color curves rise at phase 0.5, which indicates that the primary component is underfilling its Roche Lobe. This probably indicates that the primary component is not filling its Roche Lobe so we have a detached or semidetached Algol-type binary.

The 2MASS J–K = 0.452 \pm 0.046 for the binary (Cutri *et al.* 2003). This corresponds to G7.5 \pm 2.5 V eclipsing binary, which yields a temperature of 5500 \pm 250 K. Fast rotating binary stars of this type are noted for having convective atmospheres, so spots are expected. Most likely, the spots are magnetic in nature.

The B,V,R_c, and I_c curves were pre-modeled with BINARY MAKER 3.0 (Bradstreet and Steelman 2002) and fits were determined in all filter bands. The result of the best fit was that of a semidetached eclipsing binary with the secondary component filling its critical Roche lobe (classical Algol configuration). The parameters were then averaged and input into a 4-color simultaneous light curve calculation using the 2016 Wilson–Devinney program (wd; Wilson and Devinney 1971; Wilson

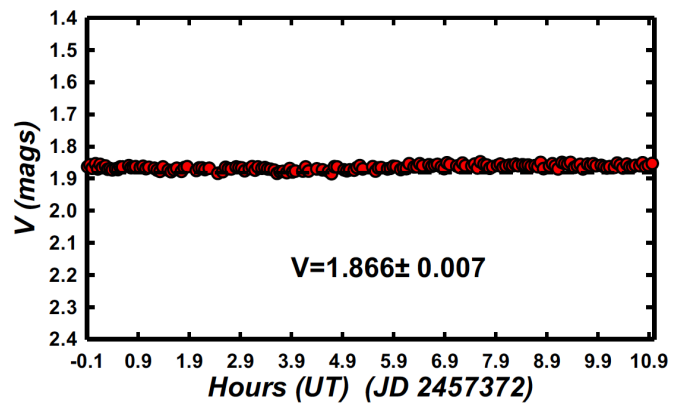


Figure 4. C–K, V magnitudes are shown on the night of JD = 2457372.

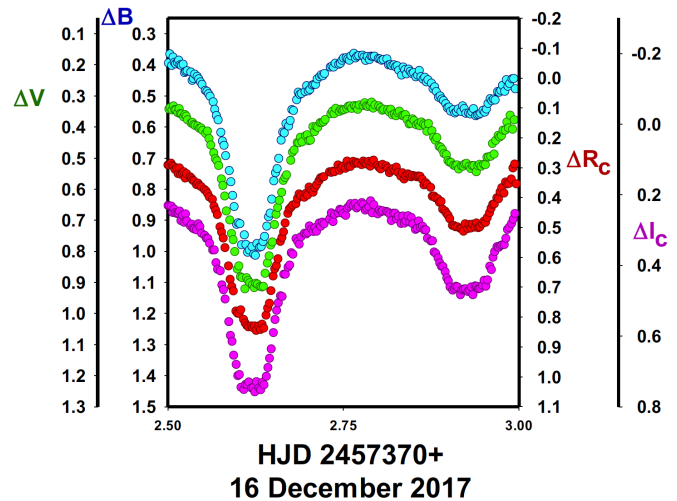


Figure 5. B,V, R_c, I_c curves on the night of December 16, 2017.

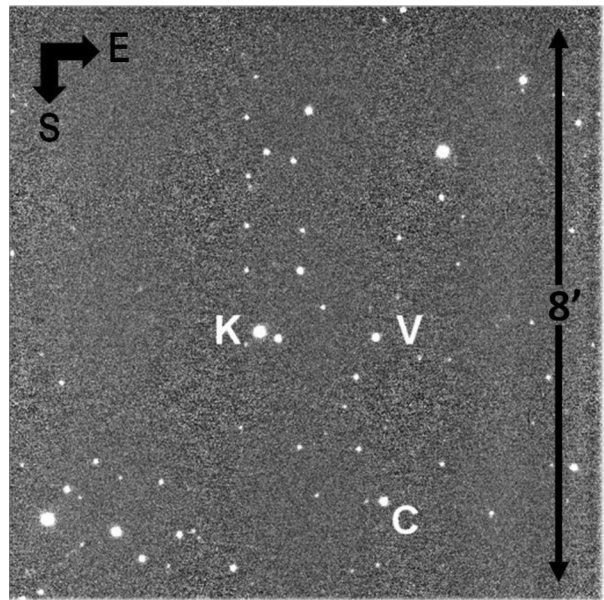


Figure 6. Finder Chart, V385 Cam (V), comparison star (C), and check (K).

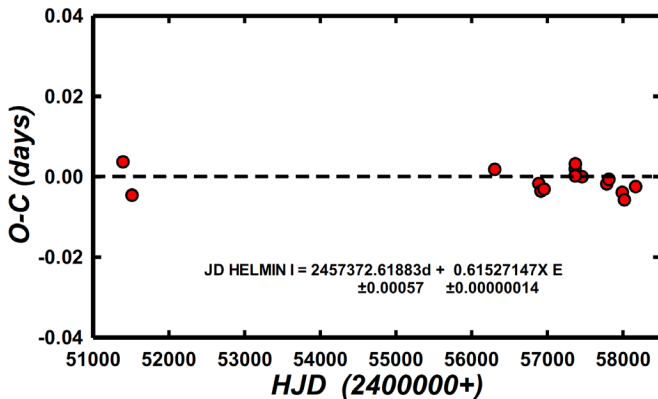


Figure 7a. The period study of 18.5 years with a linear ephemeris.

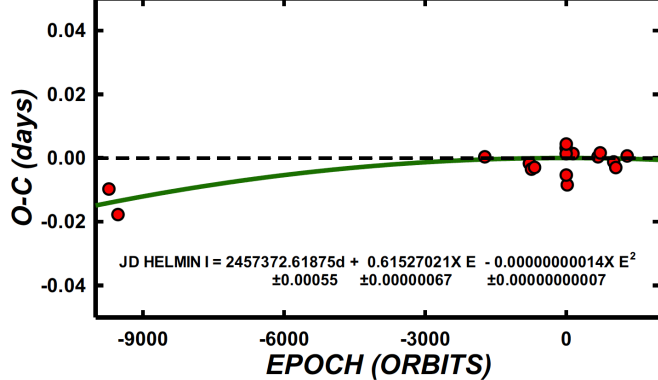
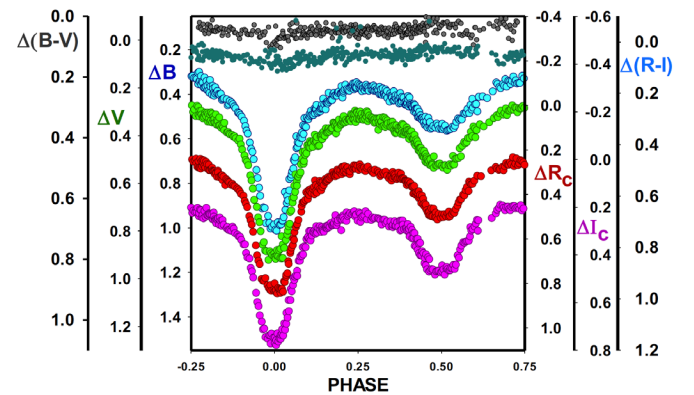
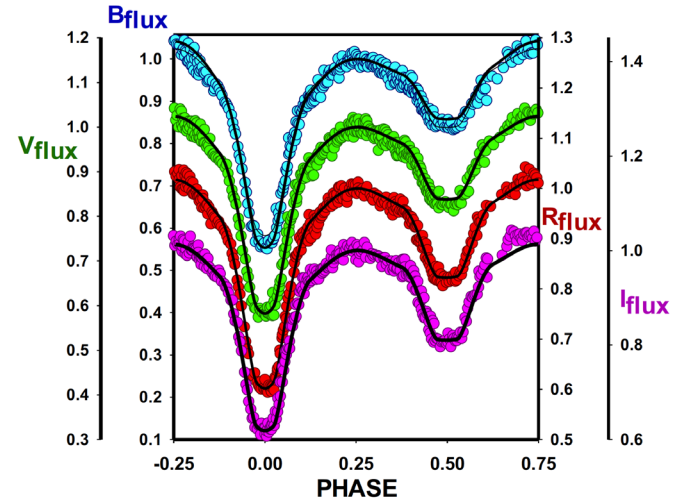


Figure 7b. The period study of 18.5 years, indicating the possibility of a continuous period decrease

1979, 1990, 1994, 2008, 2012; Van Hamme 1998; Van Hamme and Wilson 2007; Wilson *et al.* 2010; Wilson and Van Hamme 2014). The solution was computed in Mode 2 (detached) with the initial spot parameters and converged to a solution. As the referee noted, there was still an apparent O'Connell effect in the resulting solution at about the 0.75 phase. A small equatorial spot was entered about that phase and allowed to iterate along with all the other solution parameters (see Figure 9d). The model converged to a solution with the two spots, the second one at 120° colatitude with a T-factor of 1.2, and therefore is a magnetic hot spot (facula or plage). The reason for mode 2 was to allow the computation to determine the configuration. If the solution had gone detached in one or the other components the mode would have been changed to mode 4 or 5, dependent on the component that completely filled its respective Roche lobe. The computation converged in the detached mode without doing either. Convective parameters, $g = 0.32$, $A = 0.5$ were used. The spots did converge with some changes as expected.

The solution follows as Table 5. The solution was detached with the primary component nearer to critical contact potential-wise (96% fill-out) than the secondary component (91% fill-out). The binary star inclination is $\sim 85.1 \pm 0.1^\circ$, resulting in a total eclipse (secondary component) of 27.2 minutes in duration. The difference of component temperatures is about

Figure 8a. B, V, R_c, I_c light curves and color curves B-V and R-I ; magnitudes phased with Equation 2.Figure 8b. B,V,R_c,I_c normalized flux overlaid by the detached solution for V385 Cam.

980K, confirming that the components are not in contact. The modeled period was 0.61498 d.

6. Discussion

V385 Cam is a precontact W UMa binary in a detached but near contact configuration. This configuration could result, evolution-wise, in the well-known V1010 Ophiuchi configuration where the primary more massive component fills its Roche lobe first.

AML (angular momentum loss) could be in play here as indicated by its spectral type and hot spots. Its spectral type is that of a solar type with a surface temperature of 5500 K for the primary component. The secondary component has a temperature of ~ 4520 K (K4.5V). The mass ratio is 0.39, with an amplitude of 0.64–0.46 mag in B to I, respectively. The inclination is 85° which results in a total eclipse at phase 0.5.

7. Conclusion

The period study of this precontact W U Ma binary has an 18.5-year time duration. The period is found to be weakly decreasing at about the 1.5-sigma level. Decreasing periods

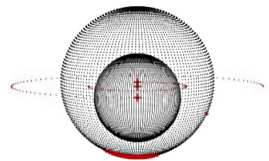


Figure 9a. V385 Cam, geometrical representation of Roche-lobe surfaces at phase 0.00.

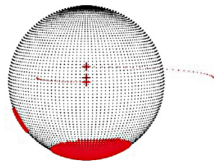


Figure 9c. V385 Cam, geometrical representation of Roche-lobe surfaces at phase 0.50.

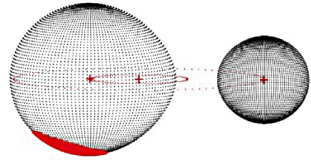


Figure 9b. V385 Cam, geometrical representation of Roche-lobe surfaces at phase 0.25.

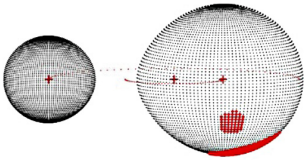


Figure 9d. V385 Cam, geometrical representation of Roche-lobe surfaces at phase 0.75.

are not unusual for a solar type binary since they can undergo magnetic braking. Conservative mass transfer from the primary component to the secondary component could also produce the same effect. The system may coalesce over time as it loses angular momentum due to ion winds moving radially outward on stiff magnetic field lines rotating with the binary (out to the Alfvén radius). The system could soon become an A-type W UMa contact binary and ultimately, one might expect that the binary will become a rather normal, fast rotating, single \sim G2V type field star after a red novae coalescence event (Tylenda and Kamiński 2016). Radial velocity curves are needed to obtain absolute (not relative) system parameters.

8. Acknowledgements

Dr. Samec would like to thank his former students for working with him over the years. Some have become professional astronomers and physicists. One of these former students, Miss Heather Chamberlain, presented a poster paper at the 2019 American Astronomical Society meeting (Chamberlain *et al.* 2019).

References

- Bailer-Jones, C. A. L., *et al.* 2013, *Astron. Astrophys.*, **559A**, 74.
 Bradstreet, D. H., and Steelman, D. P. 2002, *Bull. Amer. Astron. Soc.*, **34**, 1224.
 Chamberlain, H., Samec, R., Caton, D. B., and Faulkner, D. R. 2019, *Bull. Amer. Astron. Soc.*, **51**, 4.
- Cutri, R. M., *et al.* 2003, The IRSA 2MASS All-Sky Point Source Catalog, NASA/IPAC Infrared Science Archive (<http://irsa.ipac.caltech.edu/applications/Gator/>).
 Diethelm, R. 2013, *Inf. Bull. Var. Stars*, No. 6063, 1.
 Henden, A. A., *et al.* 2015, AAVSO Photometric All-Sky Survey, data release 9, (<https://www.aavso.org/apass>).
 Kazarovets, E. V., Samus, N. N., Durlevich, O. V., Kireeva, N. N., and Pastukhova, E. N. 2011, *Inf. Bull. Var. Stars*, No. 5969, 1.
 Khruslov, A. V. 2006, *Perem. Zvezdy Prilozh.*, **6**, 11.
 Kochanek, C. S., *et al.* 2017, *Publ. Astron. Soc. Pacific*, **129**, 104502.
 Mikulášek, Z., Chrastina, M., Liška, J., Zejda, M., Janík, J., Zhu, L.-Y., and Qian, S.-B. 2014, *Contrib. Astron. Obs. Skalnate Pleso*, **43**, 382.
 Pojmański, G. 1997, *Acta Astron.*, **47**, 467.
 Samec, R. G., Caton, D., and Faulkner, D. R. 2019, AAS Meeting #233, id.348.02.
 Samec, R. G., Olsen, A., Caton, D., and Faulkner, D. R. 2017b, *J. Amer. Assoc. Var. Star Obs.*, **45**, 148.
 Samec, R. G., Caton, D. B., Faulkner, D. R., and Hill, R. 2018, *J. Amer. Assoc. Var. Star Obs.*, **46**, 106.
 Samec, R. G., Olsen, A., Caton, D. B. Faulkner, D. R., and Hill, R. L. 2017a, *J. Amer. Assoc. Var. Star Obs.*, **45**, 173.
 Shappee, B. J., *et al.* 2014, *Astrophys. J.*, **788**, 48.
 Shaw, J. S. 1994, *Mem. Soc. Astron. Ital.*, **65**, 95.
 Tokovinin, A., Thomas, S., Sterzik, M., and Udry, S. 2006, *Astron. Astrophys.*, **450**, 681.
 Tylenda, R., and Kamiński, T. 2016, *Astron. Astrophys.*, **592A**, 134.
 U.S. Naval Observatory. 2012, UCAC-3 (<http://www.usno.navy.mil/USNO/astrometry/optical-IR-prod/ucac>).
 Van Hamme, W. V., and Wilson, R. E. 1998, *Bull. Amer. Astron. Assoc.*, **30**, 1402.
 Van Hamme, W., and Wilson, R. E. 2007, *Astrophys. J.*, 661, 1129.
 Wilson, R. E. 1979, *Astrophys. J.*, 234, 1054.
 Wilson, R. E. 1990, *Astrophys. J.*, **356**, 613.
 Wilson, R. E. 1994, *Publ. Astron. Soc. Pacific*, **106**, 921.
 Wilson, R. E. 2008, *Astrophys. J.*, **672**, 575.
 Wilson, R. E. 2012, *Astron. J.*, **144**, 73.
 Wilson, R. E., and Devinney, E. J. 1971, *Astrophys. J.*, **166**, 605.
 Wilson, R. E., and Van Hamme, W. 2014, *Astrophys. J.*, **780**, 151.
 Wilson, R. E., Van Hamme, W., and Terrell D. 2010, *Astrophys. J.*, **723**, 1469.

Table 2. V385 Cam observations, ΔB , ΔV , ΔR_c , and ΔI_c , variable star minus comparison star.

ΔB	BHJD 2457370+								
0.3550	2.4803	0.7350	2.6559	0.4400	2.8537	0.4950	3.5058	0.3390	4.9119
0.3440	2.4822	0.7020	2.6582	0.4340	2.8561	0.5070	3.5094	0.3530	4.9142
0.3390	2.4840	0.6430	2.6615	0.4190	2.8584	0.5270	3.5117	0.3500	4.9171
0.3590	2.4859	0.6170	2.6638	0.4390	2.8607	0.5230	3.5163	0.3510	4.9193
0.3490	2.4886	0.6200	2.6661	0.4470	2.8639	0.5070	3.5201	0.3180	4.9238
0.3720	2.4905	0.5900	2.6685	0.4410	2.8662	0.5270	3.5224	0.3300	4.9267
0.3720	2.4923	0.5980	2.6722	0.4560	2.8685	0.5340	3.5455	0.3200	4.9290
0.3670	2.4942	0.5800	2.6745	0.4490	2.8708	0.9680	4.4816	0.3180	4.9312
0.3620	2.4974	0.5450	2.6769	0.4600	2.8758	0.8400	4.4861	0.3280	4.9334
0.3850	2.4993	0.5480	2.6792	0.4780	2.8781	0.8580	4.4901	0.3290	4.9364
0.3950	2.5011	0.5130	2.6836	0.4720	2.8804	0.7820	4.4941	0.3320	4.9386
0.3660	2.5030	0.4890	2.6859	0.4870	2.8827	0.7620	4.4982	0.3050	4.9409
0.4030	2.5057	0.4960	2.6882	0.5050	2.8859	0.6960	4.5025	0.3010	4.9431
0.3760	2.5076	0.4930	2.6906	0.5010	2.8882	0.6840	4.5048	0.3190	4.9464
0.3930	2.5095	0.4870	2.6956	0.5110	2.8906	0.5900	4.5070	0.3440	4.9486
0.3980	2.5113	0.4680	2.6979	0.5160	2.8929	0.6380	4.5093	0.3260	4.9531
0.3930	2.5139	0.4850	2.7003	0.5260	2.8961	0.5970	4.5151	0.3830	4.9581
0.3860	2.5157	0.4800	2.7026	0.5390	2.8984	0.5730	4.5173	0.3370	4.9631
0.4010	2.5176	0.4660	2.7059	0.5370	2.9007	0.5400	4.5196	0.3630	4.9682
0.4030	2.5194	0.4640	2.7083	0.5500	2.9031	0.5080	4.5219	0.4080	4.9706
0.3990	2.5221	0.4640	2.7106	0.5450	2.9068	0.5060	4.5265	0.3700	4.9729
0.4260	2.5240	0.4460	2.7129	0.5560	2.9091	0.5130	4.5290	0.3680	5.8398
0.4220	2.5258	0.4390	2.7164	0.5520	2.9114	0.5010	4.5315	0.3520	5.8426
0.4200	2.5277	0.4330	2.7188	0.5430	2.9138	0.4760	4.5340	0.3530	5.8452
0.4240	2.5329	0.4360	2.7211	0.5510	2.9179	0.4950	4.5387	0.3750	5.8481
0.4510	2.5348	0.4290	2.7234	0.5330	2.9202	0.4650	4.5405	0.3550	5.8519
0.4450	2.5366	0.4080	2.7316	0.5420	2.9225	0.4680	4.5424	0.3600	5.8547
0.4310	2.5385	0.4050	2.7339	0.5570	2.9248	0.4490	4.5443	0.3650	5.8573
0.4380	2.5420	0.4080	2.7362	0.5560	2.9287	0.4780	4.5511	0.3640	5.8598
0.4460	2.5443	0.3960	2.7385	0.5590	2.9310	0.4600	4.5529	0.3750	5.8634
0.4560	2.5466	0.3990	2.7437	0.5520	2.9333	0.4470	4.5547	0.3590	5.8663
0.4640	2.5490	0.3960	2.7460	0.5420	2.9356	0.4210	4.5566	0.3670	5.8689
0.4830	2.5535	0.3860	2.7483	0.5650	2.9388	0.4690	4.5611	0.3860	5.8714
0.4860	2.5558	0.3790	2.7506	0.5620	2.9411	0.4400	4.5629	0.3660	5.8749
0.4940	2.5581	0.3780	2.7544	0.5600	2.9435	0.4420	4.5648	0.3650	5.8775
0.5020	2.5604	0.3820	2.7567	0.5570	2.9458	0.3950	4.5666	0.3620	5.8800
0.5200	2.5648	0.3860	2.7590	0.5470	2.9494	0.4260	4.5711	0.3700	5.8827
0.5440	2.5671	0.3720	2.7613	0.5530	2.9517	0.4270	4.5730	0.3790	5.8859
0.5640	2.5694	0.3640	2.7653	0.5430	2.9540	0.4010	4.5748	0.3870	5.8885
0.5780	2.5718	0.3790	2.7676	0.5250	2.9563	0.3950	4.5766	0.3680	5.8912
0.6180	2.5756	0.3730	2.7699	0.5100	2.9595	0.3930	4.5833	0.3790	5.8937
0.6460	2.5779	0.3710	2.7723	0.5160	2.9618	0.3890	4.5852	0.3750	5.8970
0.6600	2.5803	0.3700	2.7775	0.5110	2.9642	0.3980	4.5885	0.3980	5.8996
0.6930	2.5826	0.3760	2.7798	0.5140	2.9665	0.3650	4.5903	0.3790	5.9021
0.7410	2.5877	0.3870	2.7821	0.4870	2.9700	0.4160	4.5921	0.3870	5.9048
0.7770	2.5900	0.3740	2.7844	0.4890	2.9723	0.3940	4.5940	0.3980	5.9105
0.8210	2.5924	0.3840	2.7875	0.4830	2.9747	0.3580	4.5976	0.4100	5.9138
0.8570	2.5947	0.3730	2.7898	0.4670	2.9770	0.3660	4.6071	0.3870	5.9172
0.9140	2.5982	0.3740	2.7921	0.4860	2.9801	0.3670	4.6149	0.4060	5.9207
0.9090	2.6005	0.3730	2.7945	0.4490	2.9825	0.3470	4.6180	0.4060	5.9252
0.9120	2.6029	0.3810	2.8001	0.4700	2.9848	0.3880	4.6557	0.4140	5.9287
0.9800	2.6052	0.3820	2.8024	0.4610	2.9871	0.4220	4.8317	0.4140	5.9321
0.9480	2.6092	0.3860	2.8048	0.4460	2.9907	0.4130	4.8435	0.4160	5.9354
0.9790	2.6115	0.3840	2.8071	0.4450	2.9930	0.4110	4.8506	0.4320	5.9403
1.0040	2.6138	0.3820	2.8124	0.4780	2.9953	0.4180	4.8590	0.4090	5.9437
0.9970	2.6162	0.4010	2.8147	0.4280	3.4574	0.3880	4.8693	0.4430	5.9470
0.9860	2.6201	0.4000	2.8170	0.4420	3.4662	0.3480	4.8759	0.4550	5.9504
1.0100	2.6225	0.4040	2.8194	0.3960	3.4685	0.3550	4.8781	0.4500	5.9545
1.0140	2.6248	0.4010	2.8223	0.4210	3.4708	0.3690	4.8815	0.4660	5.9579
0.9760	2.6271	0.4070	2.8246	0.4490	3.4782	0.3740	4.8837	0.4660	5.9613
0.9880	2.6309	0.4040	2.8270	0.4410	3.4805	0.3550	4.8881	0.5060	5.9645
0.9860	2.6332	0.4180	2.8293	0.4240	3.4828	0.3630	4.8904	0.5070	5.9691
0.9700	2.6356	0.4340	2.8333	0.4150	3.4852	0.3330	4.8926	0.5130	5.9724
0.9530	2.6379	0.4080	2.8356	0.4500	3.4882	0.3670	4.8948	0.5020	5.9757
0.9200	2.6412	0.4170	2.8379	0.4620	3.4905	0.3410	4.8979	0.5260	5.9838
0.8900	2.6436	0.4300	2.8402	0.4440	3.4929	0.3440	4.9001	0.3420	5.5720
0.8780	2.6459	0.4150	2.8433	0.4500	3.4952	0.3550	4.9023	0.3510	5.5774
0.8330	2.6482	0.4220	2.8456	0.4650	3.4988	0.3410	4.9046		
0.7740	2.6512	0.4290	2.8479	0.4950	3.5011	0.3210	4.9074		
0.7480	2.6536	0.4260	2.8502	0.4800	3.5035	0.3490	4.9097		

Table continued on following pages

Table 2. V385 Cam observations, ΔB , ΔV , ΔR_c , and ΔI_c , variable star minus comparison star, cont.

ΔV	$VHJD$ 2457370+								
0.3140	2.4809	0.6600	2.6567	0.3940	2.8545	0.4530	3.5066	0.3280	4.8712
0.3210	2.4827	0.6370	2.6590	0.3900	2.8569	0.4890	3.5101	0.3160	4.8766
0.3060	2.4846	0.6110	2.6623	0.3970	2.8592	0.4940	3.5125	0.3240	4.8788
0.3130	2.4865	0.5730	2.6646	0.3850	2.8615	0.4790	3.5148	0.3080	4.8823
0.3290	2.4892	0.5630	2.6669	0.3910	2.8647	0.4970	3.5171	0.2960	4.8845
0.3230	2.4910	0.5550	2.6692	0.3950	2.8670	0.5080	3.5209	0.3130	4.8889
0.3130	2.4929	0.4690	2.6730	0.4150	2.8693	0.8960	4.4665	0.3050	4.8911
0.3200	2.4948	0.5080	2.6753	0.3900	2.8716	0.9080	4.4690	0.2870	4.8934
0.3420	2.4980	0.4820	2.6777	0.4130	2.8765	0.8810	4.4715	0.3150	4.8956
0.3310	2.4998	0.4750	2.6800	0.4340	2.8789	0.8820	4.4754	0.2970	4.8986
0.3430	2.5017	0.4510	2.6844	0.4430	2.8812	0.8760	4.4777	0.2960	4.9009
0.3380	2.5036	0.4520	2.6867	0.4350	2.8835	0.8230	4.4801	0.2900	4.9031
0.3460	2.5063	0.4340	2.6890	0.4630	2.8867	0.8570	4.4824	0.2740	4.9053
0.3330	2.5082	0.4490	2.6914	0.4660	2.8890	0.8000	4.4915	0.2930	4.9082
0.3450	2.5100	0.4290	2.6964	0.4740	2.8914	0.7210	4.4956	0.2830	4.9104
0.3460	2.5119	0.4260	2.6987	0.4860	2.8937	0.6650	4.4996	0.2850	4.9127
0.3550	2.5144	0.4450	2.7011	0.4900	2.8969	0.6110	4.5033	0.3030	4.9149
0.3420	2.5163	0.4430	2.7034	0.5090	2.8992	0.5630	4.5055	0.2860	4.9178
0.3580	2.5181	0.4000	2.7067	0.5140	2.9015	0.5920	4.5078	0.2880	4.9201
0.3590	2.5200	0.4160	2.7090	0.5150	2.9038	0.5740	4.5101	0.2860	4.9223
0.3680	2.5227	0.3990	2.7114	0.5240	2.9076	0.5210	4.5158	0.2770	4.9246
0.3610	2.5245	0.4020	2.7137	0.5260	2.9099	0.4980	4.5181	0.2850	4.9275
0.3660	2.5264	0.3870	2.7172	0.5230	2.9122	0.5190	4.5204	0.2740	4.9297
0.3780	2.5282	0.3870	2.7196	0.5360	2.9146	0.4670	4.5227	0.3020	4.9320
0.3880	2.5334	0.3840	2.7219	0.5260	2.9186	0.4410	4.5273	0.2910	4.9342
0.3860	2.5353	0.3770	2.7242	0.5270	2.9210	0.4380	4.5298	0.3190	4.9371
0.3930	2.5372	0.3580	2.7324	0.5200	2.9233	0.4240	4.5323	0.2760	4.9394
0.3960	2.5390	0.3500	2.7347	0.5180	2.9256	0.4280	4.5348	0.2810	4.9416
0.3980	2.5428	0.3580	2.7370	0.5270	2.9295	0.4230	4.5392	0.2980	4.9438
0.4050	2.5451	0.3410	2.7393	0.5350	2.9318	0.3970	4.5411	0.2970	4.9471
0.4040	2.5474	0.3510	2.7445	0.5250	2.9341	0.4210	4.5430	0.3250	4.9494
0.4120	2.5497	0.3440	2.7468	0.5250	2.9364	0.4070	4.5449	0.3050	4.9539
0.4220	2.5543	0.3470	2.7491	0.5450	2.9396	0.4050	4.5516	0.3110	4.9599
0.4140	2.5566	0.3450	2.7514	0.5250	2.9419	0.3960	4.5535	0.3040	4.9649
0.4380	2.5589	0.3410	2.7552	0.5210	2.9443	0.3900	4.5553	0.3230	4.9690
0.4590	2.5613	0.3340	2.7575	0.5270	2.9466	0.3850	4.5571	0.3300	4.9714
0.4840	2.5656	0.3330	2.7598	0.5210	2.9502	0.3700	4.5616	0.3120	4.9737
0.5030	2.5679	0.3410	2.7621	0.5220	2.9525	0.3890	4.5635	0.3370	4.9761
0.5100	2.5702	0.3320	2.7661	0.4980	2.9548	0.3750	4.5653	0.3250	4.9803
0.5250	2.5726	0.3350	2.7684	0.4970	2.9571	0.3700	4.5671	0.3470	4.9895
0.5680	2.5764	0.3440	2.7707	0.4950	2.9603	0.3710	4.5717	0.3050	5.5733
0.5890	2.5787	0.3300	2.7730	0.4540	2.9626	0.3700	4.5735	0.3130	5.5787
0.6230	2.5811	0.3320	2.7783	0.4880	2.9650	0.3460	4.5754	0.3090	5.5826
0.6710	2.5834	0.3230	2.7806	0.4440	2.9673	0.3490	4.5772	0.3150	5.8406
0.7000	2.5885	0.3330	2.7829	0.4280	2.9708	0.3920	4.5802	0.3100	5.8434
0.7440	2.5908	0.3350	2.7852	0.4330	2.9731	0.3700	4.5821	0.2960	5.8460
0.7640	2.5932	0.3320	2.7883	0.4290	2.9754	0.3710	4.5839	0.3020	5.8488
0.8020	2.5955	0.3210	2.7906	0.4110	2.9778	0.3340	4.5857	0.3110	5.8527
0.8580	2.5990	0.3400	2.7929	0.4110	2.9809	0.3560	4.5890	0.3000	5.8555
0.8480	2.6013	0.3300	2.7953	0.3850	2.9833	0.3290	4.5927	0.3100	5.8581
0.8830	2.6037	0.3330	2.8009	0.4040	2.9856	0.3190	4.5945	0.3250	5.8606
0.8860	2.6060	0.3390	2.8032	0.3630	2.9879	0.3350	4.5985	0.3080	5.8642
0.9220	2.6100	0.3470	2.8056	0.4080	2.9915	0.3330	4.6049	0.3060	5.8671
0.8860	2.6123	0.3440	2.8079	0.3780	2.9938	0.3110	4.6080	0.3040	5.8697
0.8950	2.6146	0.3450	2.8132	0.3860	3.4581	0.3150	4.6127	0.3170	5.8722
0.9020	2.6170	0.3520	2.8155	0.3770	3.4669	0.3110	4.6159	0.3240	5.8757
0.9090	2.6209	0.3440	2.8178	0.3640	3.4692	0.3050	4.6190	0.3270	5.8783
0.9180	2.6232	0.3620	2.8202	0.3620	3.4716	0.3300	4.6222	0.3330	5.8808
0.9040	2.6256	0.3590	2.8231	0.3560	3.4739	0.3080	4.6336	0.3290	5.8835
0.9070	2.6279	0.3650	2.8254	0.3870	3.4789	0.2990	4.6372	0.3290	5.8867
0.9140	2.6317	0.3550	2.8278	0.3780	3.4813	0.3770	4.6584	0.3300	5.8893
0.9160	2.6340	0.3500	2.8301	0.3790	3.4836	0.3580	4.6918	0.3270	5.8920
0.9140	2.6363	0.3640	2.8341	0.3850	3.4859	0.3800	4.7022	0.3420	5.8945
0.8720	2.6387	0.3650	2.8364	0.3830	3.4889	0.4890	4.7475	0.3240	5.8978
0.8390	2.6420	0.3610	2.8387	0.4150	3.4913	0.4880	4.7607	0.3260	5.9004
0.8160	2.6444	0.3770	2.8410	0.4100	3.4936	0.4860	4.7961	0.3320	5.9029
0.7810	2.6467	0.3910	2.8440	0.4330	3.4959	0.3710	4.8365	0.3380	5.9056
0.7710	2.6490	0.3900	2.8464	0.4250	3.4996	0.3540	4.8455	0.3450	5.9117
0.7150	2.6520	0.3750	2.8487	0.4380	3.5019	0.3630	4.8525	0.3430	5.9150
0.6820	2.6544	0.3800	2.8510	0.4520	3.5042	0.3450	4.8629	0.3580	5.9184

Table continued on following pages

Table 2. V385 Cam observations, ΔB , ΔV , ΔR_c , and ΔI_c , variable star minus comparison star, cont.

ΔV	$VHJD$ 2457370+								
ΔR	$RHJD$ 2457370+								
0.3630	5.9219	0.3880	5.9365	0.4040	5.9516	0.4530	5.9656	0.5030	5.9802
0.3670	5.9263	0.3670	5.9415	0.3980	5.9557	0.4640	5.9702	0.5000	5.9849
0.3640	5.9298	0.3920	5.9448	0.4180	5.9590	0.4660	5.9735	0.5180	5.9882
0.3520	5.9332	0.4030	5.9482	0.4420	5.9624	0.4930	5.9768		
0.2600	2.4769	0.8430	2.6321	0.2900	2.8060	0.4050	2.9712	0.3580	4.5434
0.2810	2.4813	0.8250	2.6344	0.2950	2.8113	0.3820	2.9735	0.3400	4.5502
0.2820	2.4832	0.8380	2.6368	0.3030	2.8136	0.3680	2.9759	0.3470	4.5520
0.2850	2.4850	0.7950	2.6401	0.3180	2.8159	0.3860	2.9790	0.3530	4.5539
0.2760	2.4877	0.7710	2.6424	0.3100	2.8182	0.3490	2.9813	0.3440	4.5557
0.2600	2.4896	0.7550	2.6448	0.3040	2.8212	0.3550	2.9837	0.3320	4.5602
0.2730	2.4915	0.7130	2.6471	0.3100	2.8235	0.3540	2.9860	0.3400	4.5620
0.2800	2.4933	0.6640	2.6501	0.2990	2.8258	0.3390	2.9896	0.3400	4.5639
0.2650	2.4965	0.6400	2.6524	0.3170	2.8282	0.3160	3.4523	0.3230	4.5657
0.2870	2.4984	0.6290	2.6548	0.3290	2.8322	0.3000	3.4544	0.3210	4.5703
0.2920	2.5003	0.6060	2.6571	0.3390	2.8368	0.3090	3.4565	0.3150	4.5721
0.2920	2.5021	0.5480	2.6604	0.3280	2.8391	0.3140	3.4585	0.3180	2.8345
0.2860	2.5048	0.5350	2.6627	0.3220	2.8421	0.3030	3.4651	0.3010	4.5739
0.2940	2.5067	0.5160	2.6650	0.3250	2.8445	0.3170	3.4674	0.3100	4.5758
0.2980	2.5086	0.4540	2.6711	0.3320	2.8468	0.3080	3.4697	0.3190	4.5788
0.3070	2.5104	0.4390	2.6734	0.3270	2.8491	0.3270	3.4721	0.3080	4.5806
0.3020	2.5130	0.4330	2.6757	0.3290	2.8526	0.3380	3.4771	0.2900	4.5825
0.3210	2.5148	0.4260	2.6781	0.3320	2.8550	0.3420	3.4794	0.2950	4.5843
0.3020	2.5167	0.4220	2.6825	0.3290	2.8573	0.3410	3.4818	0.3020	4.5876
0.3230	2.5185	0.4040	2.6848	0.3300	2.8596	0.3430	3.4841	0.2770	4.5913
0.3200	2.5212	0.3890	2.6871	0.3400	2.8627	0.3500	3.4871	0.2770	4.5931
0.3150	2.5231	0.3950	2.6894	0.3590	2.8651	0.3650	3.4894	0.2740	4.5961
0.3360	2.5249	0.4000	2.6945	0.3510	2.8674	0.3660	3.4918	0.2870	4.5992
0.3210	2.5268	0.3870	2.6968	0.3570	2.8697	0.3630	3.4941	0.3100	4.6056
0.3320	2.5320	0.3930	2.6991	0.3670	2.8746	0.3920	3.4977	0.2700	4.6134
0.3370	2.5339	0.3660	2.7015	0.3970	2.8770	0.3940	3.5001	0.2710	4.6166
0.3430	2.5357	0.3760	2.7048	0.3960	2.8793	0.3870	3.5024	0.2720	4.6197
0.3460	2.5376	0.3830	2.7071	0.4020	2.8816	0.4030	3.5047	0.2660	4.6244
0.3580	2.5409	0.3680	2.7095	0.4050	2.8848	0.4060	3.5083	0.4790	4.7522
0.3530	2.5432	0.3590	2.7118	0.4170	2.8871	0.4210	3.5106	0.4780	4.7886
0.3610	2.5455	0.3450	2.7153	0.4140	2.8894	0.4420	3.5130	0.3430	4.8256
0.3650	2.5478	0.3350	2.7177	0.4400	2.8918	0.4470	3.5153	0.3170	4.8407
0.3740	2.5523	0.3330	2.7200	0.4460	2.8950	0.4820	3.5190	0.3190	4.8477
0.3790	2.5547	0.3310	2.7223	0.4540	2.8973	0.4790	3.5214	0.2930	4.8665
0.3880	2.5570	0.3150	2.7305	0.4610	2.8996	0.4630	3.5253	0.2770	4.8748
0.3990	2.5593	0.3170	2.7328	0.4720	2.9019	0.4650	3.5295	0.2860	4.8770
0.4070	2.5637	0.3130	2.7351	0.4940	2.9057	0.4830	3.5335	0.2910	4.8804
0.4300	2.5660	0.3150	2.7374	0.4950	2.9080	0.8080	4.4594	0.2870	4.8827
0.4430	2.5683	0.2920	2.7426	0.4990	2.9103	0.8000	4.4670	0.2770	4.8871
0.4580	2.5706	0.3100	2.7449	0.4990	2.9127	0.8370	4.4695	0.2930	4.8893
0.4990	2.5745	0.3010	2.7472	0.5040	2.9167	0.8210	4.4735	0.2740	4.8915
0.5170	2.5768	0.2960	2.7495	0.5050	2.9191	0.8250	4.4759	0.2600	4.8938
0.5370	2.5791	0.3030	2.7532	0.5140	2.9214	0.8270	4.4782	0.2670	4.8968
0.5690	2.5815	0.2790	2.7556	0.4890	2.9237	0.8250	4.4806	0.2680	4.8990
0.6300	2.5866	0.2970	2.7579	0.5050	2.9276	0.7920	4.4843	0.2560	4.9013
0.6750	2.5889	0.2970	2.7602	0.4910	2.9299	0.7630	4.4883	0.2660	4.9035
0.6990	2.5913	0.2800	2.7642	0.5030	2.9322	0.7020	4.4923	0.2340	4.9064
0.7140	2.5936	0.2870	2.7665	0.4900	2.9345	0.6540	4.4964	0.2740	4.9086
0.7810	2.5971	0.2830	2.7688	0.5000	2.9377	0.5990	4.5015	0.2630	4.9109
0.7880	2.5994	0.2860	2.7711	0.4860	2.9400	0.5710	4.5037	0.2390	4.9131
0.7890	2.6017	0.2910	2.7763	0.5020	2.9424	0.5360	4.5083	0.2700	4.9160
0.7770	2.6041	0.2790	2.7787	0.4990	2.9447	0.4790	4.5163	0.2620	4.9182
0.8090	2.6081	0.2850	2.7810	0.4880	2.9483	0.4370	4.5186	0.2470	4.9205
0.8210	2.6104	0.2890	2.7833	0.4800	2.9506	0.4340	4.5208	0.2510	4.9227
0.8290	2.6127	0.2800	2.7864	0.4840	2.9529	0.3910	4.5253	0.2570	4.9256
0.8340	2.6150	0.2960	2.7887	0.4680	2.9552	0.3970	4.5278	0.2680	4.9279
0.8310	2.6190	0.2820	2.7910	0.4520	2.9584	0.3810	4.5303	0.2440	4.9301
0.8360	2.6213	0.2760	2.7933	0.4370	2.9607	0.3780	4.5328	0.2530	4.9324
0.8310	2.6237	0.2930	2.7990	0.4240	2.9630	0.3760	4.5377	0.2480	4.9353
0.8460	2.6260	0.3000	2.8013	0.4220	2.9654	0.3670	4.5396	0.2400	4.9375
0.8310	2.6298	0.3050	2.8036	0.4020	2.9689	0.3380	4.5415	0.2770	4.9398

Table continued on next page

Table 2. V385 Cam observations, ΔB , ΔV , ΔR_c , and ΔI_c , variable star minus comparison star, cont.

ΔR	$RHJD$ 2457370+								
ΔI	$IHJD$ 2457370+								
0.2520	4.9420	0.2460	4.9498	0.2670	4.9608	0.2970	4.9719	0.3150	4.9851
0.2410	4.9453	0.2490	4.9520	0.2810	4.9671	0.3050	4.9742	0.3590	4.9913
0.2520	4.9476	0.2540	4.9558	0.2960	4.9695	0.2940	4.9776		
0.2210	2.4773	0.7320	2.6348	0.2480	2.8116	0.3430	2.9762	0.2670	4.5706
0.2260	2.4817	0.7390	2.6371	0.2500	2.8139	0.3420	2.9794	0.2770	4.5725
0.2110	2.4835	0.7150	2.6405	0.2550	2.8163	0.3240	2.9817	0.2770	4.5743
0.2140	2.4854	0.6900	2.6428	0.2740	2.8186	0.2990	2.9840	0.2740	4.5761
0.2340	2.4881	0.6640	2.6451	0.2530	2.8216	0.2930	2.9864	0.2350	4.5791
0.2480	2.4900	0.6370	2.6474	0.2530	2.8239	0.2820	2.9899	0.2650	4.5828
0.2170	2.4918	0.5910	2.6505	0.2690	2.8262	0.2700	2.9923	0.2460	4.5879
0.2420	2.4937	0.5540	2.6528	0.2610	2.8285	0.2540	2.9946	0.2540	4.5916
0.2350	2.4969	0.5280	2.6551	0.2820	2.8325	0.2560	2.9969	0.2360	4.5934
0.2360	2.4988	0.5070	2.6575	0.2610	2.8348	0.2850	3.4547	0.2230	4.5998
0.2310	2.5006	0.4870	2.6607	0.2810	2.8372	0.2800	3.4589	0.2180	4.6140
0.2320	2.5025	0.4890	2.6630	0.2750	2.8395	0.2580	3.4678	0.2320	4.6171
0.2330	2.5052	0.4260	2.6654	0.2600	2.8425	0.2570	3.4701	0.2580	4.6203
0.2510	2.5071	0.4260	2.6677	0.2780	2.8448	0.2570	3.4725	0.2630	4.6254
0.2410	2.5089	0.4060	2.6714	0.2650	2.8471	0.2880	3.4798	0.4450	4.7759
0.2520	2.5108	0.4000	2.6738	0.2830	2.8495	0.2720	3.4822	0.4520	4.7844
0.2540	2.5133	0.3650	2.6761	0.2990	2.8530	0.2930	3.4845	0.4560	4.7916
0.2530	2.5152	0.3690	2.6784	0.2960	2.8553	0.2840	3.4875	0.2850	4.8281
0.2470	2.5170	0.3250	2.6828	0.2750	2.8576	0.2970	3.4899	0.3000	4.8418
0.2740	2.5189	0.3330	2.6852	0.2930	2.8600	0.3100	3.4922	0.2470	4.8675
0.2590	2.5216	0.3410	2.6875	0.2900	2.8631	0.3100	3.4945	0.2270	4.8751
0.2790	2.5234	0.3200	2.6898	0.3000	2.8654	0.3340	3.4982	0.2120	4.8774
0.2550	2.5253	0.3100	2.6948	0.3000	2.8678	0.3340	3.5005	0.2040	4.8808
0.2750	2.5272	0.3120	2.6972	0.3240	2.8701	0.3540	3.5028	0.1910	4.8830
0.2890	2.5324	0.3080	2.6995	0.3320	2.8750	0.3510	3.5051	0.1940	4.8874
0.2840	2.5342	0.2890	2.7018	0.3310	2.8773	0.3860	3.5087	0.2030	4.8896
0.2960	2.5361	0.2980	2.7052	0.3630	2.8796	0.3930	3.5110	0.2140	4.8919
0.2980	2.5379	0.3050	2.7075	0.3670	2.8820	0.4140	3.5134	0.2000	4.8941
0.3000	2.5412	0.2940	2.7098	0.3800	2.8852	0.3990	3.5157	0.1990	4.8971
0.2830	2.5435	0.3040	2.7121	0.3940	2.8875	0.4110	3.5195	0.2090	4.8994
0.2910	2.5459	0.2810	2.7157	0.4030	2.8898	0.4190	3.5218	0.2140	4.9016
0.3100	2.5482	0.2900	2.7180	0.4040	2.8921	0.7730	4.4597	0.2000	4.9038
0.3160	2.5527	0.2780	2.7203	0.4360	2.8977	0.7710	4.4673	0.1960	4.9067
0.3240	2.5550	0.2830	2.7227	0.4450	2.9000	0.7790	4.4698	0.1960	4.9090
0.3250	2.5574	0.2690	2.7308	0.4620	2.9023	0.7640	4.4738	0.2060	4.9112
0.3380	2.5597	0.2520	2.7331	0.4710	2.9060	0.7530	4.4762	0.2020	4.9134
0.3570	2.5640	0.2770	2.7355	0.4660	2.9084	0.7360	4.4785	0.2010	4.9164
0.3570	2.5664	0.2560	2.7378	0.4600	2.9107	0.7130	4.4809	0.2080	4.9186
0.3930	2.5687	0.2520	2.7429	0.4620	2.9130	0.6880	4.4848	0.1930	4.9209
0.4120	2.5710	0.2420	2.7452	0.4840	2.9171	0.6440	4.4889	0.2150	4.9231
0.4160	2.5749	0.2440	2.7476	0.4700	2.9194	0.5910	4.4929	0.2070	4.9260
0.4560	2.5772	0.2540	2.7499	0.4680	2.9217	0.5440	4.4969	0.2030	4.9282
0.4700	2.5795	0.2590	2.7536	0.4670	2.9241	0.4970	4.5018	0.2250	4.9305
0.4960	2.5818	0.2380	2.7559	0.4750	2.9279	0.4920	4.5041	0.2150	4.9327
0.5600	2.5870	0.2330	2.7583	0.4710	2.9302	0.4680	4.5086	0.2220	4.9356
0.5990	2.5893	0.2260	2.7606	0.4620	2.9326	0.4080	4.5144	0.2100	4.9379
0.6160	2.5916	0.2310	2.7645	0.4840	2.9349	0.4020	4.5166	0.2040	4.9401
0.6550	2.5939	0.2250	2.7669	0.4590	2.9381	0.3690	4.5189	0.2380	4.9424
0.6810	2.5975	0.2380	2.7692	0.4600	2.9404	0.3350	4.5257	0.2440	4.9479
0.7130	2.5998	0.2330	2.7715	0.4670	2.9427	0.3290	4.5282	0.2040	4.9565
0.7100	2.6021	0.2230	2.7767	0.4660	2.9450	0.3010	4.5307	0.2270	4.9615
0.7460	2.6044	0.2280	2.7790	0.4570	2.9486	0.3010	4.5332	0.2510	4.9675
0.7520	2.6084	0.2440	2.7814	0.4430	2.9509	0.3050	4.5381	0.2240	4.9699
0.7380	2.6108	0.2390	2.7837	0.4600	2.9533	0.3000	4.5400	0.2580	4.9722
0.7380	2.6131	0.2350	2.7867	0.4420	2.9556	0.2810	4.5438	0.2690	4.9746
0.7310	2.6154	0.2180	2.7891	0.4030	2.9588	0.2800	4.5505	0.2490	4.9780
0.7480	2.6194	0.2520	2.7914	0.4130	2.9611	0.2850	4.5542	0.2450	4.9812
0.7470	2.6217	0.2290	2.7937	0.3780	2.9634	0.3000	4.5561	0.2580	4.9856
0.7590	2.6240	0.2550	2.7994	0.3620	2.9657	0.2870	4.5606		
0.7300	2.6263	0.2440	2.8017	0.3480	2.9692	0.2860	4.5624		
0.7480	2.6301	0.2490	2.8040	0.3500	2.9716	0.2780	4.5642		
0.7530	2.6325	0.2460	2.8063	0.3450	2.9739	0.2870	4.5661		

Table 3. O-C residual calculations for V385 Cam.

	<i>Epoch</i> 2400000+	<i>Cycle</i>	<i>Linear</i> <i>Residuals</i>	<i>Quadratic</i> <i>Residuals</i>	<i>Weight</i>	<i>Error</i>	<i>Reference</i>
1	51396.7983	-9712.5	0.0035	0.0042	0.5	0.0010	Shaw (1994)
2	51515.8450	-9519.0	-0.0048	-0.0044	0.5	0.0010	Khruslov (2006)
3	56892.0900	-781.0	-0.0008	-0.0017	0.2	0.0100	Shappee <i>et al.</i> (2014), Kohanek <i>et al.</i> (2017)
4	56920.0830	-735.5	-0.0027	-0.0035	0.2	0.0200	Shappee <i>et al.</i> (2014), Kohanek <i>et al.</i> (2017)
5	56960.9990	-669.0	-0.0022	-0.0030	0.2	0.0200	Shappee <i>et al.</i> (2014), Kohanek <i>et al.</i> (2017)
6	57462.7560	146.5	0.0010	0.0013	0.2	0.0200	Shappee <i>et al.</i> (2014), Kohanek <i>et al.</i> (2017)
7	57789.7710	678.0	-0.0007	0.0004	0.2	0.0040	Shappee <i>et al.</i> (2014), Kohanek <i>et al.</i> (2017)
8	57817.7670	723.5	0.0004	0.0016	0.2	0.0200	Shappee <i>et al.</i> (2014), Kohanek <i>et al.</i> (2017)
9	57994.0390	1010.0	-0.0028	-0.0012	0.2	0.0200	Shappee <i>et al.</i> (2014), Kohanek <i>et al.</i> (2017)
10	58022.0320	1055.5	-0.0047	-0.0030	0.2	0.0200	Shappee <i>et al.</i> (2014), Kohanek <i>et al.</i> (2017)
11	58170.9310	1297.5	-0.0013	0.0008	0.2	0.0100	Shappee <i>et al.</i> (2014), Kohanek <i>et al.</i> (2017)
12	56309.7391	-1727.5	0.0026	0.0007	1.0	0.0007	Diethelm (2013)
13	57372.6207	0.0	0.0030	0.0030	1.0	0.0003	Present observations
14	57372.9266	0.5	0.0012	0.0013	1.0	0.0011	Present observations
15	57374.4678	3.0	0.0042	0.0043	0.5	0.0043	Present observations
		r.m.s.	0.00278	0.00266			

Table 4. Light curve characteristics for V385 Cam.

<i>Filter</i>	<i>Phase</i>	<i>Magnitude</i>	$\pm \sigma$	<i>Phase</i>	<i>Magnitude</i>	$\pm \sigma$
	0.25	Max. I		0.75	Max. II	
B		0.365	0.010		0.323	0.009
V		0.318	0.015		0.289	0.015
R		0.279	0.008		0.249	0.008
I		0.236	0.012		0.218	0.007

<i>Filter</i>	<i>Phase</i>	<i>Magnitude</i>	$\pm \sigma$	<i>Phase</i>	<i>Magnitude</i>	$\pm \sigma$
	0.5	Min. II		0.0	Min. I	
B		0.556	0.013		1.002	0.013
V		0.532	0.012		0.902	0.011
R		0.507	0.006		0.837	0.006
I		0.467	0.012		0.691	0.020

<i>Filter</i>	<i>Min. I -</i>	$\pm \sigma$	<i>Max. I -</i>	$\pm \sigma$	<i>Min. I -</i>	$\pm \sigma$
	Max. I		Max. II		Min. II	
B	0.637	0.023	0.043	0.019	0.446	0.025
V	0.583	0.026	0.030	0.031	0.370	0.023
R	0.558	0.014	0.030	0.016	0.330	0.011
I	0.456	0.032	0.018	0.019	0.224	0.032

<i>Filter</i>	<i>Max. I -</i>	$\pm \sigma$	<i>Min. II -</i>	$\pm \sigma$
	Max. II		Max. I	
B	0.356	0.010	0.191	0.023
V	0.303	0.015	0.213	0.027
R	0.271	0.008	0.228	0.014
I	0.229	0.012	0.231	0.024

Table 5. B,V,R_c,I_c Wilson-Devinney program solution parameters.

<i>Parameters</i>	<i>Values</i>
$\lambda_{B^*}, \lambda_V, \lambda_R, \lambda_I$ (nm)	440, 550, 640, 790
g_1, g_2	0.32
A_1, A_2	0.5
Inclination (°)	85.16 ± 0.09
T_1, T_2 (K)	5500, 4520 ± 3
Ω_1, Ω_2	2.7717 ± 0.0020, 2.913 ± 0.002
$q(m_2/m_1)$	0.3904 ± 0.0007
Fill-outs: F_1, F_2 (%)	96.0 ± 0.1, 91.3 ± 0.1
$L_1 / (L_1 + L_2 + L_3)_I$	0.8756 ± 0.066
$L_1 / (L_1 + L_2 + L_3)_R$	0.8909 ± 0.067
$L_1 / (L_1 + L_2 + L_3)_V$	0.9100 ± 0.075
$L_1 / (L_1 + L_2 + L_3)_B$	0.9327 ± 0.077
JD _o (days)	2457372.6204 ± 0.0001
Period (days)	0.61498 ± 0.00007
$r_1/a, r_2/a$ (pole)	0.4147 ± 0.0015, 0.2387 ± 0.0010
$r_1/a, r_2/a$ (point)	0.4994 ± 0.0047, 0.2673 ± 0.0048
$r_1/a, r_2/a$ (side)	0.4385 ± 0.0020, 0.2448 ± 0.0030
$r_1/a, r_2/a$ (back)	0.4590 ± 0.0026, 0.2589 ± 0.0039
Spot 1 (Star 1)	
Co-Latitude	161.37 ± 0.03
Longitude	192.5 ± 0.1
Radius	31.80 ± 0.09
T-factor	1.151 ± 0.001 (6134 ± 33 K)
Spot 2 (Star 1)	
Co-Latitude	119 ± 2
longitude	97.54 ± 0.03
Radius	9.952 ± 0.002
T-factor	1.200 ± 0.006 (6134 ± 33 K)